Proceedings of CONF-FMCE 2025 Symposium: Semantic Communication for Media Compression and Transmission
DOI: 10.54254/2755-2721/155/2025.GL23375

Effect of Diffusion Welding Parameters on the Microstructure and Mechanical Properties of Al-9.6at%Sc/6061Al Dissimilar Joints

Lu Zhang[123], Xiaowei Zhang[123*], Daogao Wu[12], Dongyang Tang[1234], Lulu Wu[123], Senhui Wang[1234]

[1]National Engineering Research Center for Rare Earth, Grirem Advanced Materials Co., Beijing, China
[2]Grirem Hi-Tech Co., Ltd., Langfang, China
[3]General Research Institute for Nonferrous Metals, Beijing, China
[4]School of Metallurgy and Environment, Central South University, Changsha, China
**Corresponding Author. Email: 04202095@163.com*

Abstract: The fundamental physical properties of the Al-9.6at%Sc alloy were experimentally determined, and diffusion welding experiments on Al-9.6at%Sc targets were performed. The results of the study revealed the following key findings: For the Al-9.6at%Sc alloy, the average coefficient of thermal expansion is 28.3×10^{-6} /℃ (within the range of 25~520 ℃), the average thermal conductivity is 161 W/(m·K) (25~600 ℃), Young's modulus decreases from 93 GPa at 25 ℃ to 74 GPa at 600 ℃, the density is 2.66 g/cm³, and the specific heat capacity is 1.05 J/(g·K). In diffusion welding of Al-9.6at%Sc alloy to a 6061Al alloy backing plate, as the maximum residual stress at the interface is only 19.62 MPa. In the hot isostatic pressing diffusion welding process, a high-strength joint can be obtained when the surface roughness is below 0.8 μm, the welding temperature is maintained between 450 and 500℃, the welding pressure is around 125 MPa, and the holding time ranges from 3 to 5 hours. Furthermore, Mg atoms from the 6061Al alloy accumulate around the Al_3Sc phase in the Al-9.6at%Sc alloy, forming stable Mg-Al solid solutions at the weld joint.

Keywords: Al-9.6at%Sc alloy target, numerical simulation, residual stress, diffusion welding, welding strength

1. Introduction

Aluminum-scandium (AlSc) targets play a crucial role in the high-power magnetron sputtering process used for the fabrication of AlScN thin films. The piezoelectric coefficient of AlScN films with a scandium content of 43 at% is significantly enhanced to 27.6 pC·N-1, compared to 6.9 pC·N-1 for films without Sc incorporation [1-4]. As a result, AlSc targets are widely used in the production of 5G RF filters.

During the fabrication process of 5G RF filters, there is a reliability issue under high-power sputtering for the conventional brazed target, of that the brazing material may melt and result in delamination from the backing plate. Therefore, some efforts have been made to explore the welding of AlSc target, such as Yao [5] employed spraying technique to form a backing plate, and prepared

DOI: 10.54254/2755-2721/155/2025.GL23375

AlSc target through multi-step treatment and machining, but the welding strength was not reported, Jia [6] sprayed Al or Cu alloy on the AlSc alloy surface to form backing plate, the welding strength exceeded 70 MPa after heat treatment, Cao [7] used direct casting method to prepare AlSc target, and the welding strength was over 10 MPa. Up to now, there are some problems on the AlSc target prepared by above methods, such as low welding strength, poor interfacial quality, high porosity, severe oxidation, and so on. Diffusion welding method, with the advantages of high welding strength, avoiding defects such as porosity, segregation and cracks, it is very suitable for AlSc target welding [8,9].

2. Methods

2.1. Materials preparation

High-purity scandium (99.99% purity) and 5N-grade commercial high-purity aluminum were used as raw materials in this experiment. Al-9.6at%Sc alloy was prepared using a vacuum induction furnace, and cylindrical samples with a diameter of 50 mm and a thickness of 8 mm were cut by wire electrical discharge machining (EDM). A larger Al-9.6at%Sc alloy target, with a diameter of 330 mm and a thickness of 8 mm, was also fabricated by EDM. In the hot isostatic pressing (HIP) diffusion welding process, key factors influencing joint quality include surface roughness, welding pressure, and holding time.

2.2. Experiment procedure

HIP diffusion welding process begins with preparing the materials to ensure clean, smooth surfaces. The materials are then assembled according to design specifications, sealed in a metal container, and subjected to a vacuum to remove air. The sealed assembly is placed in the HIP system, where it is gradually heated to the predetermined temperature while uniform isostatic pressure is applied. Once target conditions are reached, the temperature and pressure are maintained for a specified time to enable diffusion bonding. After welding, both temperature and pressure are gradually reduced, and the assembly is removed for final machining and surface treatment to meet dimensional requirements.

2.3. Testing methods

The Al-9.6at%Sc alloy was polished, cleaned with deionized water and anhydrous ethanol, and dried with cold air. Microstructural and compositional analyses were performed using a Leica DMI3000-M optical microscope and a JSM-IT700HR scanning electron microscope (SEM). Phase identification was conducted using a Rigaku Smartlab 9 kW X-ray diffractometer with Co Kα radiation. Thermal expansion was measured with a DIL402SE dilatometer, and thermal diffusivity and specific heat capacity were obtained via the flash method using an LFA467HT system. Thermal conductivity was calculated accordingly, and density was determined by the Archimedes method.

Advanced microstructure characterization was carried out using a JSM-7610 Plus SEM (20 kV) and a Talos F200 X TEM. Chemical composition was analyzed by energy-dispersive spectrometry (EDS). Tensile tests were performed on a WDW-100 universal testing machine at 25°C with a crosshead speed of 4.2 mm/min and a strain rate of 2.5×10^{-4} s^{-1}. Fracture surfaces were examined in both SE and BSE modes using SEM. Surface roughness was measured with an HT-180 profilometer.

For bonding strength evaluation, Al-Sc target samples were machined and tested according to GB/T 228.1 standards. The bonding area (S) was calculated based on specimen dimensions, and bonding strength was determined from the failure load (Fm) using a universal testing machine. Each sample consisted of three replicates, and average values were reported.

DOI: 10.54254/2755-2721/155/2025.GL23375

3. Diffusion welding experiment results

3.1. Determination of physical parameters

Table1 summarizes the physical properties of the Al-9.6at%Sc alloy measured in this study. The coefficient of thermal expansion (CTE), tested from 20℃ to 520℃, increased from 14.03×10^{-6}/℃ at 25℃ to 31.95×10^{-6}/℃ at 520℃, with an average of 26.97×10^{-6}/℃. The CTE curve shows a sharp rise between 25℃ and 30℃, a slower increase up to 200℃ indicating microstructural stabilization, and a linear growth from 200℃ to 520℃. Thermal conductivity, measured from 20℃ to 600℃, decreased slightly from 170 W/(m·K) at 25℃ to 164.2 W/(m·K) at 600℃, averaging 162.74 W/(m·K). Young's modulus declined linearly from 91 GPa at 25℃ to 51 GPa at 450℃, then more gradually to 71 GPa at 600℃, with an average of 83.2 GPa. Table 2 compares these properties with those of common backing plate materials, including 304 stainless steel, oxygen-free copper, CuCr alloy, molybdenum, CuZn alloy, and CuNi alloy. Among them, 6061 Al alloy exhibits comparable thermal and mechanical properties, making it a favorable backing plate candidate for Al-Sc alloy bonding.

Table 1: Physical properties of Al-9.6at%Sc alloy

Material	T/℃	E/GPa	C/(J/(g*k))	CTE/(10^{-6}/℃)	K/(W/(m*K))	ρ_S/(g·cm^{-3})
Al-9.6at%Sc	20	91	0.897	14.03	170	2.68
	100	89	0.920	25.77	165	
	200	87	0.940	25.73	167	
	300	84	0.960	27.64	163	
	400	82	0.980	29.78	159	
	500	79	1.000	31.78	158	
	520	71	1.070	31.95	156	

Table 2: Physical properties of common backing plate materials

Material	ρ_S/(g·cm^{-3})	CTE/(10^{-6}/℃)	C/(J/(g*K))	K/(W/(m*K))	Refs.
6061Al	2.75	27.8	0.855	166	[10,11]
304 steel	7.93	16.2	0.5	21	[12]
OFC	8.96	20.05	0.385	395	[13]
CuCr	8.7	17.5	0.395	205	[14]
Mo	10.22	4.8	0.250	138	[15]
CuZn	8.5	19.5	0.390	120	[16,17]
CuNi	8.6	17.3	0.395	38	[17,18]

3.2. Effect of surface roughness on welding strength

Fig.1 presents the SEM and XRD images of the Al-9.6at%Sc alloy. The microstructure of the Al-9.6at%Sc alloy consists of the α-Al phase and a second phase, the second phase exhibits irregular large particles predominantly distributed evenly in the α-Al matrix. Base on the XRD results, the second phase is Al_3Sc, so that, when the Sc content is 9.6at.%, the alloy primarily consists of the α-Al phase and the Al_3Sc phase (gray particles pointed by white arrow in Fig.1(a)). Table 3 lists the composition of second phase by EDS analysis, the average Al content is 25.45 at%, and the average Sc content is 74.55 at%, the atomic ratio of Al to Sc is about 3, it is agreed with the XRD results.

DOI: 10.54254/2755-2721/155/2025.GL23375

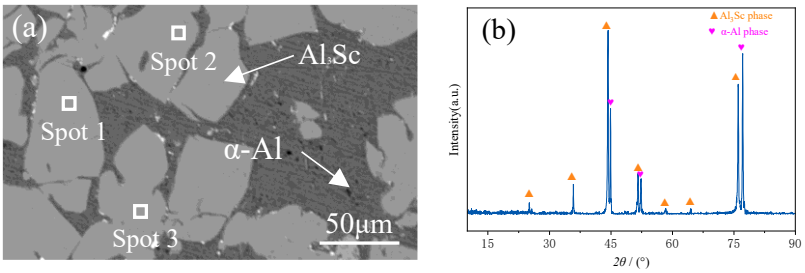

Figure 1: Al-9.6at%Sc alloy (a)SEM image, (b)XRD pattern

Table 3: EDS point scan results of Al_3Sc phase in Al-9.6at%Sc alloy

	Spot 1	Spot 2	Spot 3	Average
Al/%	74.69	74.03	74.93	74.55
Sc/%	25.31	25.97	25.07	25.45

Fig.2 shows the influence of surface roughness on the welding interface and strength. At 450 ℃ and 100 MPa, a surface roughness of ~0.8 μm enhances contact area and diffusion, yielding an average welding strength of 90.3 MPa. As roughness increases to 1.6 μm, contact area decreases, limiting diffusion and reducing strength to 54.01 MPa. For roughness ≥2 μm, bonding further deteriorates, with strength dropping to 45.43 MPa or resulting in failed joints.

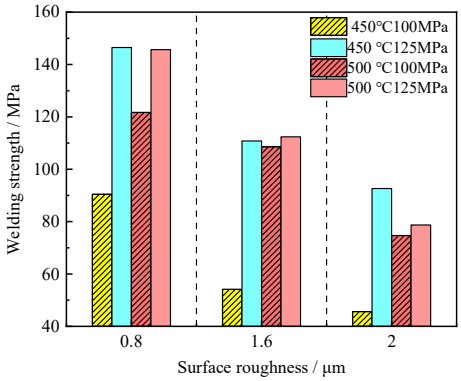

Figure 2: Effect of surface roughness on welding strength

Fig.3 presents SEM images of the welded interface at 480 ℃ and 100 MPa. In Fig.3(a), with a surface roughness of ~2 μm, a 5 μm-wide crack is observed at the interface, indicating poor bonding and low welding strength. In Fig.3(b), at ~1.6 μm roughness, a discontinuous crack (~0.25 μm) appears, and the average strength is 53.5 MPa. In contrast, Fig.3(c) shows a smooth, crack-free interface at ~0.8 μm roughness. A surface roughness below 0.8 μm enhances interfacial contact and atomic diffusion while reducing stress concentrations, thereby improving welding strength.

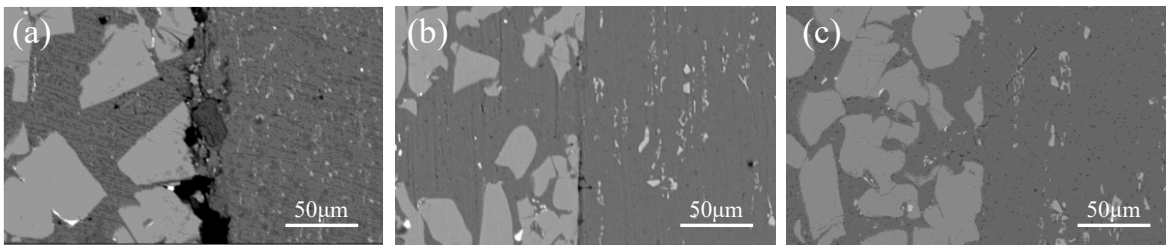

Figure 3: SEM images of welded samples processed at 480℃ and 100 MPa

DOI: 10.54254/2755-2721/155/2025.GL23375

(a) surface roughness of 2 μm, (b) surface roughness of 1.6 μm and (c) surface roughness of 0.8 μm

3.3. Effect of pressure on welding strength

Welding strength of Al-9.6at%Sc alloy and backing plate after 3 h with welding pressure of 70 MPa to 150 MPa is shown Fig.4. At the pressure of 70 MPa, there is no effective bonding achieved between the Al-9.6at%Sc alloy and the backing plate at 450℃ and 500 ℃. At 450℃, the samples show an average welding strength of 89.9 MPa under 100 MPa pressure, 147 MPa under 125 MPa pressure, and 89.5 MPa under 150 MPa pressure. When the temperature is increased to 500 ℃, the average welding strength rises to 123 MPa at 100 MPa pressure, 145 MPa at 125 MPa pressure, and reaches 90.2 MPa at 150 MPa pressure.

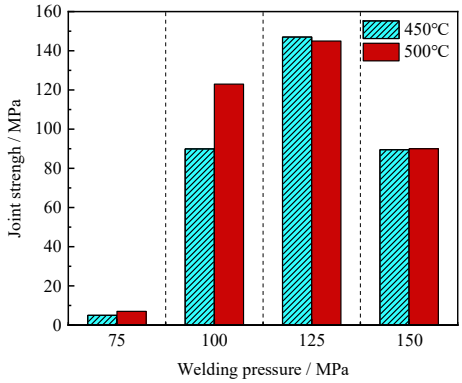

Figure 4: Effect of pressure on Al-9.6at%Sc target welding strength

The SEM images of the welding interface after 3 h at 450 ℃ under the pressure of 125 MPa and 150 MPa are shown in Fig.5, the welding interface is tightly bonded with high connection strength. When the welding pressure is 150 MPa, as seen in Fig.5(b), there are some fragmented of Al_3Sc phase appeared at welding interface.

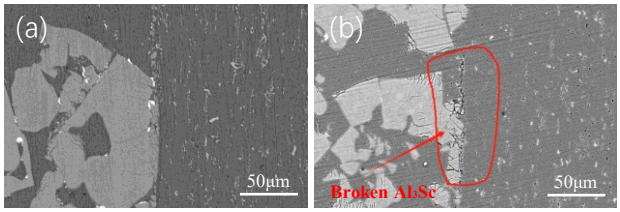

Figure 5: SEM images of the welding interface of t samples after 3-h insulation at 450℃ (a)125 MPa, (b) 150 MPa

Fig.6 shows SEM images of the fracture surfaces of tensile samples tested at 480 ℃ for 3 h under applied stresses of 125 MPa and 150 MPa. In Fig.6(a), the fracture surface under 125 MPa exhibits well-defined ductile dimples, indicating a ductile fracture mode and strong interfacial bonding. In contrast, Fig. 6(b) reveals that at 150 MPa, the increased stress leads to fracture within the Al_3Sc phase at the bonding interface. Cracks initiate at the Al_3Sc/α-Al interface and propagate along it. The fracture surface displays a fine river-like pattern, and point scanning analysis confirms that the fractured region is primarily composed of Al_3Sc, identifying it as the weakest zone under high-stress conditions.

DOI: 10.54254/2755-2721/155/2025.GL23375

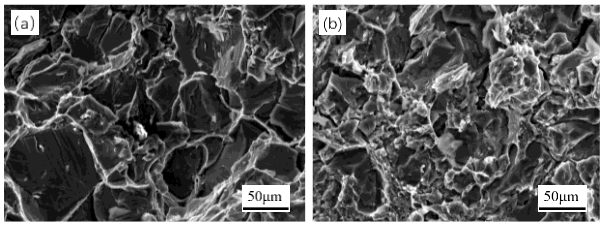

Figure 6: SEM images of the fracture surface of t samples after 3-h insulation at 450℃ (a) 125 MPa, (b) 150 MPa

The experimental results demonstrate that welding pressure is a critical factor influencing interfacial bonding quality. At low welding pressures, the dense surface oxide layer remains intact, impeding the diffusion welding process and resulting in weak interfacial bonding without atomic-level contact. Conversely, at high welding pressures, the hard and brittle Al_3Sc phase may fracture under stress, and the resulting fragments disperse along the interface, thereby reducing the overall weld strength.

3.4. Effect of holding time on welding strength

Holding time is a critical factor in the HIP diffusion welding process. When the welding temperature is 450 ℃ and pressure is 125 MPa, the effective bonding between the Al-9.6at%Sc alloy and the 6061Al alloy backing plate is failed to achieve with 2 h holding time, the localized atomic diffusion is incomplete, and the Al-9.6at%Al target is easy to crack and delaminate. As shown in Fig.7, when the holding time extends to 5 h at the same welding temperature and pressure, the atomic diffusion at is sufficient, leading to the formation of a high-strength weld joint.

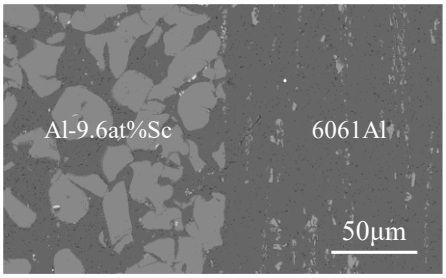

Figure 7: SEM image of the welding interface at 450℃, 125 MPa, after a 5 h holding time

3.5. Effect of welding temperature on welding strength

Fig.8 presents the welding strength for the Al-9.6at%Sc alloy and 6061Al alloy backing plate after 3 h holding period. At the temperature of 400 ℃, the welding strength is in the range of 8.77 MPa to 15.3 MPa, it is result in the risk of target delamination under the pressure of 100 MPa, 125 MPa and 150 MPa. At the temperature of 450 ℃, the welding strength increases significantly, it increases to the range of 93.39 MPa to 117.19 MPa, when the welding strength between the target and the backing plate exceeds 30 MPa, the welding of the target can be considered safe and reliable. At the temperature of 500 ℃, the average welding strength further increases, reaching 145.51 MPa.

DOI: 10.54254/2755-2721/155/2025.GL23375

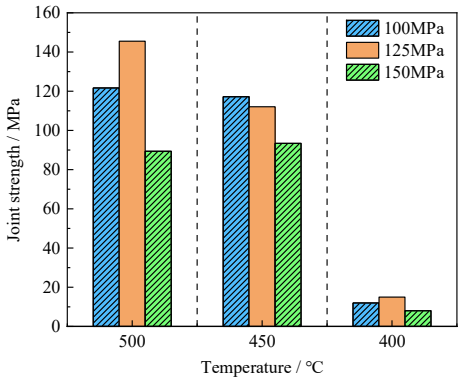

Figure 8: The effect of welding temperature on welding strength among different samples

Fig.9 shows the SEM images of the welding interface of the diffusion-welded target under a welding pressure of 125 MPa. In Fig.9(a), discontinuous unbonded cracks are observed at the welded interface at a welding temperature of 400℃, indicating insufficient diffusion and incomplete bonding. In Fig.9(b) 450℃, the welding surface is fully bonded with no visible cracks, indicating adequate diffusion between the Al-9.6at%Sc alloy and the 6061Al alloy backing plate, effectively eliminating gaps and achieving atomic-level bonding.Based on the experimental results, the optimal welding temperature range is between 450℃ and 500℃. At temperatures above 500℃, the 6061Al alloy backing plate softens or melts, resulting in uneven joints and reduced welding strength. Additionally, high temperatures may induce oxidation or other chemical reactions that degrade the welding quality. At 400 ℃, slow atomic diffusion leads to insufficient bonding, weakening the welding strength and potentially introducing microcracks or defects. Therefore, the optimal welding temperature for bonding the Al-9.6at%Sc alloy and 6061Al alloy backing plate is between 450℃ and 500℃.

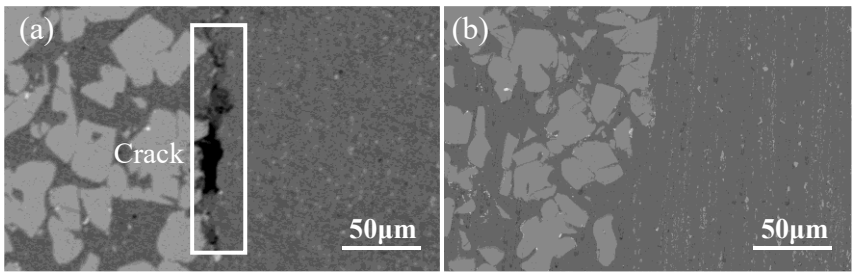

Figure 9: SEM images of the welding interface of Al-9.6at%Sc target under 125 MPa pressure (a) 400℃ and (b) 450℃

4. Conclusions

The residual stress distribution in the diffusion welding process of the Al-9.6at%Sc alloy and 6061Al alloy were investigated in this study, while the fundamental physical properties of Al-9.6at%Sc was also tested experimentally. Additionally, the effects of surface roughness at the welding interface, welding pressure, welding temperature and holding time on the welding quality were studied systematically. The main conclusions are summarized as follows:

(1) The physical parameters of Al-9.6at%Sc alloy are tested experimentally, the coefficient of thermal expansion increases from 14.03×10^{-6}/℃ at 25℃ to 32.95×10^{-6}/℃ at 520℃, the thermal conductivity decreases from 170 W/(m·K) at 25℃ to 156 W/(m·K) at 600℃, the Young's modulus is 93GPa at 25℃, reducing to 74 GPa at 600℃. the measured density was 2.66 g/cm³, and the specific heat capacity was 1.05 J/(g·K).

DOI: 10.54254/2755-2721/155/2025.GL23375

(2) The welding strength exhibits an increasing trend with reduction surface roughness, and the highest average welding strength of the weld joint is achieved when the surface roughness is below 0.8 μm.

(3) In the temperature range of 450~500℃, the average welding strength of the Al-9.6at%Sc target reaches a maximum of 146.49 MPa.

(4) The average welding strength of Al-9.6at%Sc target reaches a maximum of 145.51 MPa with the optimal welding pressure being 125 MPa

(5) Alloying elements in the sample were sufficiently diffused when the holding time is 3-5 h, the average welding strength maintains above 120 MPa.

Acknowledgments

Project supported by the National Key R&D Program of China (2022YFB3504402).

References

[1] *Milena M, Johan B, Ilia K, Ventsislav Y. Aluminum scandium nitride thin-film bulk acoustic resonators for wide band applications. Vacuum, Volume 86, Issue 1, 4 July 2011, 23-26.*

[2] *Akiyama M, Umeda K, Honda A, et al. Influence of scandium concentration on power generation figure of merit of scandium aluminum nitride thin films. Applied Physics Letters, 2013, 102(2).*

[3] *Men K, Liu H, Wang X, et al. AlScN films prepared by alloy targets and SAW device characteristics. Journal of Rare Earths, 2023, 41(3): 434-439.*

[4] *Wang X, Wang Y, He J, Ding Z, Luo J, Hui S. Application and research progress of AlSc material for high frequency filter.Chin J Rare Met. 2023;47(2):303.*

[5] *Yao LJ, Pan J, Wang XZ, Chen YJ. A Forming Method for Al-Sc Alloy Target: CN201711302847.5[P].2019-11-05.*

[6] *Jia Q, Cao XM, Jiao XK, Li LL, Zhang XN, Hu HL, et al. A Low-Segregation Al-Sc Alloy Target and Its Preparation Method: CN202210514946.4[P].2024-05-17.*

[7] *Cao XM, Ding ZC, Li YJ, Jia Q, Li LL, Qu P, et al. A One-Step Forming Preparation Method for Diffusion-Welded AlSc Alloy Target: CN202011617741.6[P].2022-06-17.*

[8] *Xu, GJ, Luo JF, Wan XY, ,Li YJ, Xiong XD, Teng HT, et al. Research on Diffusion Welding Technology of High Purity Rare Earth Yttrium Target and Copper Alloy Backing plate. Rare Metals, 2023, 44(02): 71-76.*

[9] *Enjyo T, Ikeuchi K, Kanai M, Maruyama T. Diffusion welding of aluminum to titanium. Trans. JWRI, 1977, 6(1): 123-130.*

[10] *Y. Mishin, J. Mehl, D.A. Papaconstantopoulos, et al. Structural stability and lattice defectsin copper: Ab initio, tight-binding, and embedded-atom calculations. Physical Review B, 2001,63:224106.*

[11] *Li J Z, Wang Q, Zhang P. Numerical Simulation of the Temperature Field in Friction Stir Welding of Dissimilar Metals: 6061 Aluminum Alloy/AZ31 Magnesium Alloy. Hot Working Technology, 2024, 53(09): 59-63*

[12] *Jiang H, Ying ZP, Liu JP, Hu CB. Numerical Simulation of Friction Stir Welding of Dissimilar Aluminum Alloys A356/6061. Modeling and Simulation, 2023, 12: 5103.*

[13] *Su X P, Luo G Q, Shen Q, Zeng H, Wang CB, Zhang L M et al. Research on Vacuum Diffusion Bonding of TC4/OFC. Rare Metal Materials and Engineering, 2010(11): 2044-2047.*

[14] *Xiao J. Numerical Simulation and Optimization Design of W-Cu-Ti Diffusion Bonding Process. Wuhan University of Technology, 2012.*

[15] *Garber M, Scott BW, Blatt FJ. Thermal Conductivity of Dilute Copper Alloys. Physical Review, 1963, 130(6): 2188.*

[16] *Shi, C , Li HD, and Zhou L . Materials Science and Engineering, Vol. 1. Chemical Industry Press, 2004.*

[17] *Li M, Zinkle S J. Physical and mechanical properties of copper and copper alloys[J]. 2012.*

[18] *Jiao SY, Dong JX, Zhang MC, Xie XS. Study on the Interdiffusion Behavior of Reaction Layer Elements in Hot Isostatic Pressing Diffusion Welding of Corrosion-Resistant Alloys and Carbon Steel. Materials Engineering, 2009, (12): 10-16.*